

# Automatika

Journal for Control, Measurement, Electronics, Computing and Communications



ISSN: (Print) (Online) Journal homepage: <https://www.tandfonline.com/loi/taut20>

## Voltage and reactive power correlation in multi-objective optimization of an offshore grid

Muhammad Raza

To cite this article: Muhammad Raza (2021) Voltage and reactive power correlation in multi-objective optimization of an offshore grid, *Automatika*, 62:3-4, 454-470, DOI: [10.1080/00051144.2021.1984632](https://doi.org/10.1080/00051144.2021.1984632)

To link to this article: <https://doi.org/10.1080/00051144.2021.1984632>



© 2021 The Author(s). Published by Informa UK Limited, trading as Taylor & Francis Group.



Published online: 30 Sep 2021.



Submit your article to this journal [↗](#)



Article views: 349



View related articles [↗](#)



View Crossmark data [↗](#)



# Voltage and reactive power correlation in multi-objective optimization of an offshore grid

Muhammad Raza

Department of Electrical Engineering, Bahria University, Karachi Campus, Karachi, Pakistan

## ABSTRACT

In the last few years, many offshore wind power plants are installed at North Sea and more are under construction. Offshore grid would be vital in the integration of future offshore wind power plant with the main land grid. Both, multi-terminal DC and AC cable systems are under consideration in the concept of future offshore grid. The reactive power and voltage operating point for such a network is important for the optimized operation. This article presents an optimization criterion of voltage and reactive power control for an offshore AC grid having a parallel connecting grid-forming converter. Multi-objective optimization problem is formulated considering four reactive power management strategies. The solution of the optimization algorithm is analysed and compared with respect to active power losses in the network, voltage variation, and reactive power contribution by the sources. The research presents a methodology to apply a suitable reactive power management strategy to achieve the best optimum operating points. The solution provides the optimum operating points for offshore wind farm reactive power, frequency and voltage droop gain values for VSC-HVDC system, and reactive power sharing factor of HVDC transmission.

## ARTICLE HISTORY

Received 24 June 2020  
Accepted 17 September 2021

## KEYWORDS

Droop control;  
multi-objective optimization;  
offshore wind power plants;  
offshore AC hub; reactive  
power management;  
VSC-HVDC transmission  
system

## 1. Introduction

The development of technologies associated with the offshore wind farm have grown significantly in the past 10 years. The capacity of a single wind turbine has now reached up to 12 MW i.e. Haliade-X. In 2018, newly installed turbines rated capacity was 6.8 MW in average which is 15% larger than in 2017 [1]. Increase in a wind turbine capacity also enables the development of larger offshore wind farms. The average size of offshore wind farm has also increased from 79.6 MW (2017) to 561 MW (2018) [1]. Wind farm developers are exploring favourable conditions deep into the sea to increase the wind farm generation capacity. In 2018, two projects were commissioned located almost 103 km from shore i.e. Hornsea One and EnBW Hohe See [1]. In Europe, the ambition of increasing offshore wind energy share in the state electricity generation will require the development of meshed offshore grid.

The concept of offshore grid at North and Baltic sea will evolve gradually from the existing single point radial connection into cross-border meshed HVAC/HVDC grid [2]. The offshore grid techno-economic study considering the aspects of technical, economic, policy, and regulatory concludes that the offshore hub connection will be highly beneficial [3]. A hub could be an AC or DC offshore substation where different offshore wind farms located in close proximity are connected to each other. The combined power

from this hub can then be transferred to shore using a single transmission line. A similar concept, namely “Hub and Spoke”, is proposed for the interconnected transmission system at North Sea by Tennet in which an artificial island will be built in the centre of different offshore wind farms that are far from shore but near to this island. These offshore wind farms will be connected to this island using HVAC cables and HVDC transmission will be used to export power to onshore grids [4]. This island will be able to connect numerous wind farms with a total capacity of over 30 GW [4].

The VSC-HVDC transmission systems will play a vital role in the realization of the future offshore grid [5]. The VSC abilities to control the active and reactive power independently, black start, and frequency support are the distinct features that open the new ways of designing offshore wind farm layout as well as export system [6–11]. A concept of collection system for offshore wind farm topology is presented to build the pure DC power system [12, 13]. In the DC collection system, the wind turbines contain only turbine side converter and they are connected in series, called string, to raise the DC voltage of the transmission line. Strings are connected in parallel to integrate the wind farm power, and the accumulated power is transferred to onshore grid [14, 15]. Some variants of DC collection system may also include the DC-DC converter at offshore to raise the voltage from medium to high which increases

the power transfer capability [16–19]. However, the string voltage is difficult to control within the limited variation band due to wind variations. Also, successful operation of such network highly relies on the DC protection system [20, 21]. In mesh offshore grid, the DC network formulation at the level of wind farm would be complex and sensitive to system changes. It employs an expensive protection scheme and requires high reliability. Alternatively, offshore AC network will have mature technology equipment especially AC circuit breaker, and HVDC system based interconnected transmission system will be comparatively simple to develop [22]. The offshore network energized by multiple grid-forming converters will have redundancy of distributed slack sources. These grid-forming converters also contribute in optimal operation of the offshore AC network [23–25].

Offshore network optimal operation is an essential requirement of transmission operators and wind farm developers to ensure maximum profit [26–29]. This is achieved by determining optimal operating points using an optimization algorithm according to objectives and constraints. The prime object in the optimization algorithm is to minimize the active power losses [30]. The operating points for an offshore wind farm connected with a VSC-HVDC transmission system are reactive power dispatch by grid side converter of wind turbine systems and reference voltage set-point of HVDC transmission system offshore converter [31–33]. The regulation of reactive power flow consequently impacts the network voltages. Offshore grid is considered to be a weak network since the VSC power rating is slightly higher than the combined power ratings of all the wind turbines. Large voltage deviation in a weak grid from its nominal value will cause voltage instability consequently wind turbine will be disconnected. Thus, static voltage stability is also required to be considered in the objective function [34]. Multi-objective optimization is nowadays widely applied to find the optimal solution to fulfil several operational requirements. However, these objective functions conflict with each other and provide an optimal solution for only one objective, while compromising others [35, 36]. Multi-objective optimization problem can be handled by different methods such as goal programming algorithm, simplex method,  $\epsilon$ -constraints, and weighted sum [37]. In all such methods, Pareto-efficient points are usually determined graphically to select the best compromised solution.

AC voltage droop scheme in a grid-forming converter enables control of the reactive power sharing among offshore HVDC transmission systems. An optimization algorithm can be applied to determine the desired voltage droop gain according to the power sharing criteria [24]. However, unregulated reactive power will flow depending on the droop gain value. Thus, additional constraints need to be defined to ensure

network operation within limits. Furthermore, planners and developers choose the reactive power management criteria according to the operational requirement thus the optimization solution is also influenced by these criteria. These criteria are based on network operational requirement such as set-point of a busbar voltage magnitude, reactive power dispatch, and active power export. Thus, it is important to analyse the difference in optimization results and decide the most suitable criteria according to the operational requirement.

The presented work is a continuation of the previous work given in [24, 25]. In [24], reactive power management strategy is proposed for the selection of voltage droop gain using an optimization algorithm. The article only demonstrates the methodology and analysis of the proposed criteria, and its implementation in an offshore meshed grid. In [25], integration of offshore AC grid and meshed DC network is addressed. The article focuses on the design and operation of Multi-terminal DC network and DC voltage droop gain selection. In [25], it is demonstrated that the offshore grid can be integrated successfully with the multi-terminal DC grid using the proposed criterion.

The objective of the presented article is to analyse the effects of reactive power management strategies on the network optimization. Currently, no such study is performed for the optimization of the offshore AC grid having parallel connected grid-forming converters considering different reactive power management strategies. This article presents a methodology to apply a suitable strategy to achieve the best optimum operating points for an offshore AC grid. In the article, novel reactive power management strategy is compared with other strategies, and network operation is analysed to comprehend strategies impacts. Moreover, a non-trivial multi-objective optimization problem is formulated that compares four different strategies for reactive power sharing and voltage droop gain selection. An interior-point method is applied to attain the optimized results and select the best reactive power management strategy. The rest of the paper is organized as follows: Section 2 explains the VSC-HVDC control system and the strategies of reactive power management in the offshore AC network, Section 3 describes the implementation of optimization algorithm, the analysis of the optimization results have been performed in Sections 4, and 5 concludes this paper.

## 2. Methodology

A possible offshore AC network configuration interconnecting two offshore grids is shown in Figure 1. The analysis is aimed to draw conclusions based on realistic data therefore the network configuration is derived from offshore wind farms installed at North Sea. The energy from offshore wind farms Albatros, Deutsche

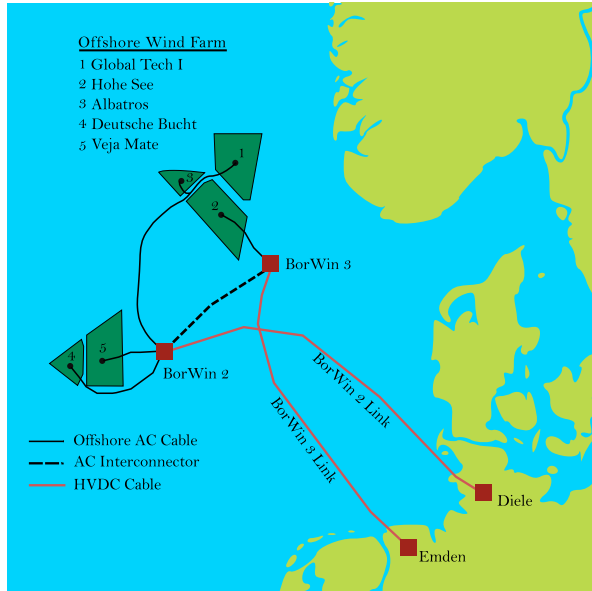


**Figure 1.** Offshore AC network configuration interconnecting two offshore substations.

Bucht, Global Tech-I, and Veja Mate are transferred to onshore through BorWin2 HVDC link. Offshore wind farm Hohe See is connected with BorWin3 offshore substation. Furthermore, it is expected that the grid connection of Global Tech-I wind farm will be shifted from BorWin2 to BorWin3 in future [38]. The offshore converters of BorWin2 and BorWin3 HVDC transmission system operate as grid-forming converters which provide the reference frequency for the offshore AC network and energize it. Wind farms are synchronized to this reference frequency and feed energy into the network. The wind farms layout is in radial or radial-ring configuration therefore the energy flows from wind farms to HVDC link.

The AC cable connection between BorWin2 and BorWin3 offshore substation is not under consideration at the present moment. In the present scenario, the unavailability of any one HVDC link, due to schedule maintenance and fault, will stop the energy infeed into the grid from the respective wind farms. The presented research considers the cable between both offshore HVDC converter substations since the future offshore grid will have parallel connected grid-forming converters. These converters are the offshore side converters of the HVDC transmission systems, and they are connected together via HVAC cable. This enhances the trade, improves network contingency, and gives provision to control network reference voltage through multiple sources.

### 2.1. VSC-HVDC offshore converter control

The control of parallel connected grid-forming converters employs the frequency and voltage droop

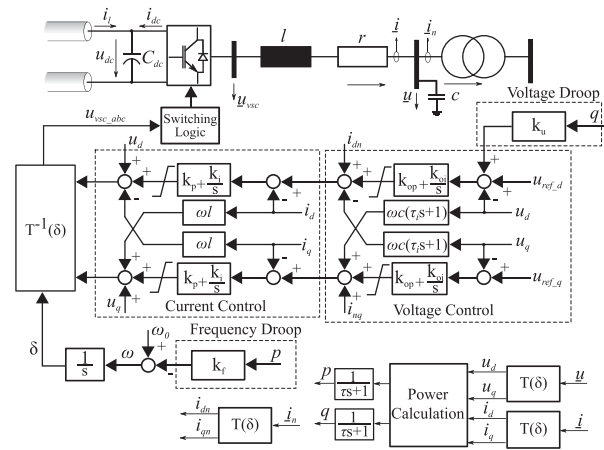


**Figure 2.** VSC-HVDC offshore converter control structure.

scheme as a tertiary level control to enable the control over the active and reactive power flow sharing among themselves. Offshore side converter control structure of VSC-HVDC transmission system is shown in Figure 2. The control system has three levels of control i.e. inner current control loop, outer voltage control, and tertiary level droop control. The design of current and voltage control is discussed in [22]. The dynamic aspects of frequency and voltage droop control loops for parallel connected grid-forming converters are discussed in [39]. In this article, emphasis is given to the steady-state aspect of tertiary level droop control.

In the offshore AC network, all the grid-forming converters act as the reference machine. The net active power infeed by the wind turbines must be received by these grid-forming converters, and the total received power sharing among the converters can be controlled by adjusting droop gain value [24]. The setting of power sharing can be according to the energy export requirement. The sharing criteria can be added as a constraint to the optimization algorithm to get the desired droop value. The solution of the optimization algorithm also provides the reactive power sharing factor of grid-forming converters considering the converter operating limits.

### 2.2. VSC-HVDC onshore converter control

HVDC transmission system is in point-to-point configuration, therefore onshore side converter must control the DC voltage to balance the transmission line. The control structure of onshore converter is shown in Figure 3. The design of onshore converter control is discussed in [10]. The research is focused on the optimization of offshore AC network, therefore onshore network is not modelled in detail and represented by an equivalent grid. However, the losses of onshore converters are considered in the optimization algorithm. The onshore converters are set in the DC voltage and reactive power control mode.



the network. The optimal operating points of elements that control the reactive power flow are determined by defining an optimization problem. In the power system optimization problem, the network characteristics are defined as equality and inequality constraints, whereas, active power loss equation is defined as an objective function. Optimization considering only active power loss often deviates the network voltages from its rated value, therefore, voltage deviation is considered as the second objective function. In this article, interior-point optimization method is applied in MATLAB to determine solution using multiple initial values.

A nonlinear optimization problem can be defined in MATLAB using function “fmincon”. This function supports different nonlinear programming solvers such as interior-point method, sequential quadratic programming (SQP), and trust-region-reflective method. Each solver has its own advantage and disadvantage, however, among them interior-point method is the most effective. It finds the minimum of the objective function within the boundary of nonlinear multivariable constrained functions considering multiple initial values. The optimization problem can be defined as:

$$\min_x f(x) \text{ such that } \begin{cases} c(x) \leq 0 \\ ceq(x) = 0 \\ lb \leq x \leq ub \end{cases} \quad (2)$$

Here,  $f(x)$  is a nonlinear objective function that returns a scalar quantity,  $c(x)$  is the vector of nonlinear inequality function,  $ceq(x)$  is the vector of nonlinear equality function, and  $lb$  and  $ub$  are the vectors of lower and upper boundary of the state variable  $x$ . The system nonlinear equations and state variable boundary conditions are explained in the subsequent sections.

### 3.1. Objective functions

Multi-objective optimization functions are usually conflicting in nature and require trade-off between them in order to obtain the favourable solution. Weighted sum method is the simplest approach to achieve the trade-off among several objective functions. In this method, a weighting factor is assigned to each objective function as expressed by Equation (3). The optimal operating points and the best solution can then be determined using Pareto Front analysis.

$$\min \{F(x)\} \\ F(x) = \sum_{m=1}^n \gamma_m f_m(x) \quad \gamma_m \in [0, 1] \quad (3)$$

Here,  $\gamma_m$  is the weight of the  $m$ th objective function and  $n$  is the total number of objective functions. In general, the weights are selected to satisfy Equation (4).

$$\sum_{m=1}^n \gamma_m = 1 \quad (4)$$

In the presented study, two objective functions are selected for the optimization problem. Here,  $\gamma$  is assigned to first objective function and the second objective function weight factor would be  $(1 - \gamma)$ .

The first objective function is active power loss which is expressed by Equation (5). The function is defined as the least square error of the network active power losses.

$$f_1(p) = \left( \sum_{i=1}^y p_i + \sum_{j=1}^z p_j \right)^2 \quad (5)$$

Here,  $p_i$  is the active power infeed of the  $i$ th offshore wind farm, and  $p_j$  is the active power received at the  $j$ th onshore grid. The full weight to this objective function is given at  $\gamma = 1$ .

The network bus voltage least square error is defined as the second objective function which is expressed as Equation (6).

$$f_2(v) = \sum_{i=1}^k (u_i - 1.0)^2 \quad (6)$$

Here,  $u_i$  is the voltage magnitude of the  $i$ th bus. The full weight to this objective function is given at  $\gamma = 0$ . The functions are defined in p.u system. Pareto optimal solution of the multiple objective functions can be obtained from Equation (7) as a single objective optimization problem.

$$\min \{f(p, v, \gamma)\} \\ f(p, v, \gamma) = \gamma \cdot f_1(p) + (1 - \gamma) \cdot f_2(v) \quad (7)$$

### 3.2. Constraints

System definition, network configuration and power management control conditions are defined as constraints in the optimization problem. These constraints consist of nonlinear equalities and inequalities mathematical expressions which define the network topology, power sharing condition, operational boundary limits, and reactive power management strategies.

#### 3.2.1. Network topology

Network topology can be defined using power flow equations as equality constraint in the optimization algorithm. The offshore network comprises of AC and DC transmission systems. The power flow equation for each busbar in the AC network can be defined using Equation (8).

$$p_l = u_l \sum_{m=1}^{nb} u_m (g_{lm} \cos(\delta_l - \delta_m) + b_{lm} \sin(\delta_l - \delta_m)) \\ q_l = u_l \sum_{m=1}^{nb} u_m (g_{lm} \sin(\delta_l - \delta_m) - b_{lm} \cos(\delta_l - \delta_m)) \quad (8)$$

Here,  $nb$  is the total number of AC busbars in the offshore network,  $p_l$  and  $q_l$  are the active and reactive power at the  $l$ th AC bus respectively,  $u_l$  and  $u_m$  are the AC busbar effective voltages,  $\delta_l$  and  $\delta_m$  are the voltage angle of the AC busbars, and  $g_{lm}$  and  $b_{lm}$  are the conductance and susceptance of the branch elements in the AC network.

Only active power flows in the DC network. Thus, only active power flow equation can sufficiently define the DC network configuration. The DC active power at any  $i$ th busbar can be defined using (9).

$$P_i = U_i \sum_{j=1}^k U_j G_{ij} \quad (9)$$

Here,  $k$  is the total number of DC busbars.  $P_i$  is the DC active power at the  $i$ th busbar,  $U_i$  and  $U_j$  are the DC voltages, and  $G_{ij}$  is the conductance of the branch elements between  $i$ th and  $j$ th busbars.

The converter losses are calculated as the function of steady-state current using Equation (10).

$$P_{loss} = a + b \cdot i_{vsc} + c \cdot i_{vsc}^2$$

$$i_{vsc} = \frac{\sqrt{p_{vsc}^2 + q_{vsc}^2}}{u_{vsc}} \quad (10)$$

Here,  $q_{vsc}$  is the reactive power of the offshore converter,  $u_{vsc}$  is the offshore converter busbar voltage,  $a$  is a no-load coefficient,  $b$  is the voltage drop coefficient, and  $c$  is the ohmic loss coefficient. These coefficients are derived from [40] and are given in Table A3. The converter equations are completed by defining the active power loss function as Equation (11).

$$p_{vsc} + P_{dc} + P_{loss} = 0 \quad (11)$$

Here,  $p_{vsc}$ , and  $P_{dc}$  are the AC and DC active power of the offshore converter,  $P_{loss}$  is the active power loss in the converter.

### 3.2.2. Active and reactive power sharing factor

With the application of frequency and voltage droop schemes, the transmission system operators can have the additive control over the active and reactive power sharing among HVDC transmission systems. The droop gain values are calculated by defining the active and reactive power sharing factor.

Consider  $\alpha$  as the active power sharing factor of the total active power ( $p_s$ ). For  $n$  grid-forming converters in the offshore network, the active power for each VSCs can be calculated using Equation (12).

$$\begin{aligned} p_1 &= \alpha_1 \cdot p_s \\ p_2 &= \alpha_2 \cdot p_s \\ &\vdots \\ p_n &= \alpha_n \cdot p_s \end{aligned} \quad (12)$$

The sum of all the grid-forming VSCs must be equal to the net active power infeed by the wind farms, thus Equation (12) can be simplified as Equation (13).

$$p_s = p_1 + p_2 + \dots + p_n$$

$$p_s = \left( \sum_{i=1}^n \alpha_i \right) p_s \quad (13)$$

$$\sum_{i=1}^n \alpha_i = 1 \quad \forall \alpha \in \mathfrak{N} : 0 \leq \alpha \leq 1$$

The  $n$ th VSC sharing factor must be defined as Equation (14) in order to satisfy the condition given in Equation (13).

$$\alpha_n = 1 - \sum_{i=1}^{n-1} \alpha_i \quad (14)$$

The relationship between the active power sharing factor and the frequency droop gain can be defined using Equation (15).

$$\alpha_i = \frac{1}{k_{f-i}} \cdot \frac{1}{\sum_{j=1}^n \frac{1}{k_{f-j}}} \quad (15)$$

Here,  $\alpha_i$  and  $k_{f-i}$  are the active power sharing factor and droop gain value of the  $i$ th converter,  $k_{f-j}$  is the droop gain value of the  $j$ th converter, and  $n$  is the total number of the converter.

To determine the frequency droop values, Equation (15) is implemented in the optimization algorithm for  $n-1$  converters. To fulfil the condition given in Equation (14), the  $n$ th VSC power sharing condition must be defined using Equation (16) in the algorithm.

$$p_n \left( \sum_{i=1}^{n-1} \alpha_i \right) - \left( 1 - \sum_{i=1}^{n-1} \alpha_i \right) \sum_{i=1}^{n-1} p_i = 0 \quad (16)$$

Similarly,  $\beta$  is defined as the reactive power sharing factor. The reactive power of all converters can be defined as Equation (17).

$$\begin{aligned} q_1 &= \beta_1 \cdot q_s \\ q_2 &= \beta_2 \cdot q_s \\ &\vdots \\ q_n &= \beta_n \cdot q_s \end{aligned} \quad (17)$$

Here,  $q_s$  is the sum of the reactive power flow of all converters. Also, condition given in Equation (18) needs to be satisfied.

$$q_s = q_1 + q_2 + \dots + q_n = \sum_{i=1}^n \beta_i q_i \quad (18)$$

$$\sum_{i=1}^n \beta_i = 1 \quad \forall \beta \in \mathfrak{R} : 0 \leq \beta \leq 1$$

To determine the voltage droop gain value, Equation (19) is implemented in the optimization algorithm.

$$(1 - \beta_i) q_i - \beta_i \sum_{\substack{j=1 \\ j \neq i}}^n q_j = 0 \quad (19)$$

### 3.2.3. Upper and lower boundary limits

The network upper and lower operational limits are set as inequality constraints in the optimization algorithm. These operational limits are based on the general requirements of the grid codes and are applied as Equation (20).

$$\begin{aligned} u_{k,\min} &\leq u_k \leq u_{k,\max} \\ q_{wf,\min} &\leq q_{wf} \leq q_{wf,\max} \\ q_{vsc,\min} &\leq q_{vsc} \leq q_{vsc,\max} \\ p_{vsc,\min} &\leq p_{vsc} \leq p_{vsc,\max} \\ k_{f,\min} &\leq k_f \leq k_{f,\max} \\ k_{u,\min} &\leq k_u \leq k_{u,\max} \\ 0 &\leq \beta \leq 1 \end{aligned} \quad (20)$$

Here,  $k$  is the index of the busbar and 10% tolerance is allowed on the network busbar voltage  $u_k$ . The reactive power limits at the wind farm connection point,  $q_{wf,\min}$  and  $q_{wf,\max}$ , corresponds to 0.98 PF at full load. The converters reactive power limits,  $q_{vsc,\min}$  and  $q_{vsc,\max}$ , corresponds to the 0.9 PF at the rated capacity. The converters active power limits,  $p_{vsc,\min}$  and  $p_{vsc,\max}$ , are also applied according to the export capacity of the transmission line. The frequency and voltage droop gain limits,  $k_{f,\min}$ ,  $k_{f,\max}$ ,  $k_{u,\min}$ , and  $k_{u,\max}$  are set according to the stability limits [39].

In addition, the maximum frequency deviation at maximum power is defined as (21).

$$p_{\max} - \Delta\omega_{\max} \sum_{i=1}^n \frac{1}{k_{f,i}} < 0 \quad (21)$$

Here,  $p_{\max}$  is the net active power export capacity,  $i$  is the index of the offshore converters,  $k_f$  frequency droop gain value,  $n$  total number of grid-forming converters in the offshore network,  $\Delta\omega_{\max}$  is the maximum allowed frequency deviation.

### 3.2.4. Reactive power management strategies

In addition to above-mentioned constraints, reactive power control conditions are also implemented

as equality constraints according to reactive power management strategies. In MS1 strategy, no voltage droop scheme and reactive power sharing factor equation are applied. The converter controls the bus voltage using Equation (22).

$$u_i - 1.0 = 0 \quad (22)$$

Here,  $i$  is the index of the converter. In MS2 strategy, voltage droop scheme is applied with reactive power sharing factor as discussed in the previous section. In MS3 strategy, all the wind farm PCC busbars are regulated at rated voltage using Equation (23) along with the droop scheme.

$$u_{wf,j} - 1.0 = 0 \quad (23)$$

Here,  $j$  is the index of wind farm PCC bus. In MS4, the reactive power exchange condition among the grid-forming converters are defined using Equation (25). The condition implies that any change in reactive power due to droop gain in one converter must be balanced with the change in reactive power with other converters. This can be understood by the droop effect on the load bus as Equation 24.

$$q_l - u_l \underbrace{\sum_{\substack{m=1 \\ m \neq i}}^{nb-1} u_m h_{lm} - u_l u_0 h_{li}}_{k_{u,i}=0} - \underbrace{u_l k_{u,i} q_i h_{li}}_{\Delta q_{k,i}} = 0 \quad (24)$$

Here,  $h_{lm} = g_{lm} \sin(\Delta\delta_{lm}) - b_{lm} \cos(\Delta\delta_{lm})$ , and  $h_{li} = g_{li} \sin(\Delta\delta_{li}) - b_{li} \cos(\Delta\delta_{li})$ .

The reactive power mismatch equation in case of no droop scheme can be defined by first three terms in Equation (24). The droop gain equation changes the reference bus voltage as the function of converter reactive power ( $\Delta q_{k,i}$ ). This additional reactive power must be absorbed by network or active devices in the system. Since, this reactive power is produced due to VSC control scheme, the criteria given in Equation (25) can be applied to determine the droop gains so that this additional reactive power exchanges among the grid-forming converters.

$$\begin{aligned} \Delta q_{k_1} + \Delta q_{k_2} + \dots + \Delta q_{k_z} &= 0 \\ \sum_{i=1}^z \sum_{l=1}^y u_l k_{u,i} q_i h_{li} &= 0 \quad \forall i, l : i \neq l \end{aligned} \quad (25)$$

Here,  $z$  is the total number of grid-forming VSCs in the offshore AC network,  $y$  is the total number of load buses connected with the  $i$ th VSC.

## 4. Case studies

Network operators and planners determine the optimize operational set-point to minimize the network losses and voltage deviation according to certain criteria. These criteria are based on network operational

requirement such as set-point of a busbar voltage magnitude, reactive power dispatch, and active power export. Network operation could be more optimized depending on the one criteria or another. The criteria defines the management of the reactive power in the network. Thus in this section, comparison of reactive power management strategies is demonstrated through two case studies. In the first case study, a small network is considered to analyse the objective function minimization as a function of wind turbine reactive power dispatch while keeping all other parameters constant. In the second case study, proposed methodology is applied on the network based on several offshore wind farms and optimized results are analysed considering the variation of active power sharing factor, wind turbine active power output variation, and objective function weighting factor. In both case studies, two objective functions are considered i.e. active power losses and network voltage deviation.

#### 4.1. Offshore AC network having one offshore wind farm

As discussed in previous sections, the future offshore grid would be the combination of multiple VSC-HVDC transmission lines connecting different onshore grids to one or more offshore wind farms. A simplified example of such a network is illustrated in Figure 4. A single offshore wind farm is connected to two VSC-HVDC systems. Power flow would be positive in the direction of arrow. In this example optimization only focuses offshore network therefore DC network and onshore grids are not required to model. A simple optimization problem is to determine the reactive power set-point of the wind turbines. In this case study, wind farm is set to supply rated active power i.e. 100 MW. Both converters rated active power capabilities are 100 MW as well, thus full active power can be transferred to onshore via only one transmission line. Active power sharing between HVDC transmission lines is controlled by  $\alpha$ . Here,  $\alpha$  is set to 0.5 which means both HVDC transmission lines are transferring 50 MW to onshore. Further, wind farm has the capability to supply  $\pm 40$  MVar reactive power. The base power for the calculation is 200 MVA.

The percentage change in an active power loss of the network using MS1, MS2, and MS3 strategies with respect to MS4 strategy is illustrated in Figure 5. For

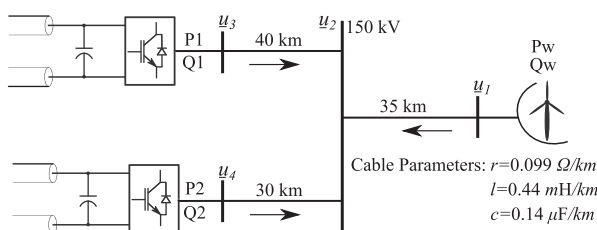


**Figure 4.** Offshore AC network with one offshore wind farm.

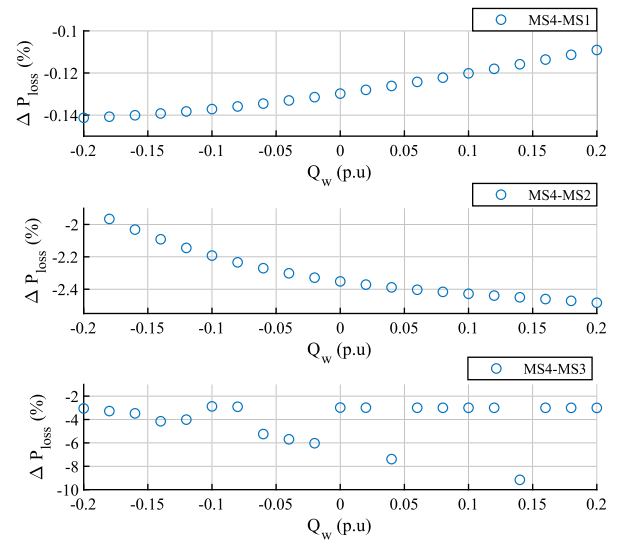


**Figure 5.** Active power loss comparison between proposed criteria with respect to other, when  $\gamma = 0.5$  and  $\alpha = 0.5$ .

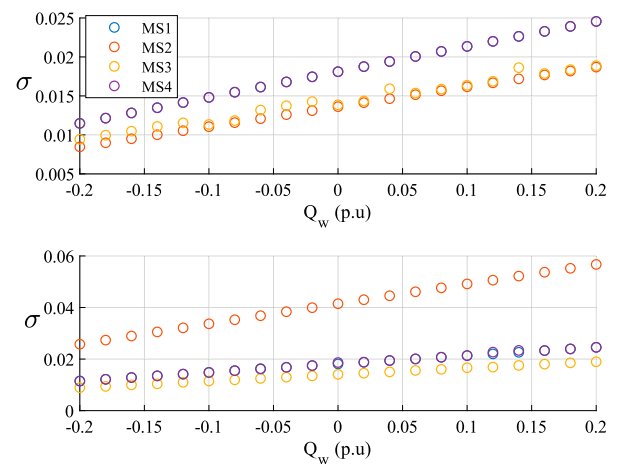


**Figure 6.** Voltage standard deviation with  $\mu = 1.0$  p.u., when  $\gamma = 0.5$  (top) and  $\gamma = 1.0$  (bottom).

this result, both objective functions have equal weightage i.e.  $\gamma$  is set to 0.5. The diagram shows that the network has more losses using MS1, MS2, and MS3 reactive power strategies in comparison with MS4 strategy, i.e. active loss in the network would be 0.14% more with MS1 strategy in comparison with MS4 at  $-0.2$  p.u. wind farm reactive power set-point. Note that only wind farm reactive power is changed while keeping all other parameters constant.

In Figure 6, comparison of network voltages standard deviation is illustrated for all reactive power management strategies. The standard deviation is calculated with respect to rated busbar voltage by setting  $\mu = 1.0$  p.u. This indicates that how much network voltages deviate from the rated value in each strategy. When  $\gamma = 0.5$ , both MS1 and MS4 strategies will give higher voltages in the network in comparison with MS2 and MS3. However, MS1, MS3, and MS4 will have the lowest voltage deviation at  $\gamma = 1.0$ . Moreover, it is clear that network voltages are within the tolerance range

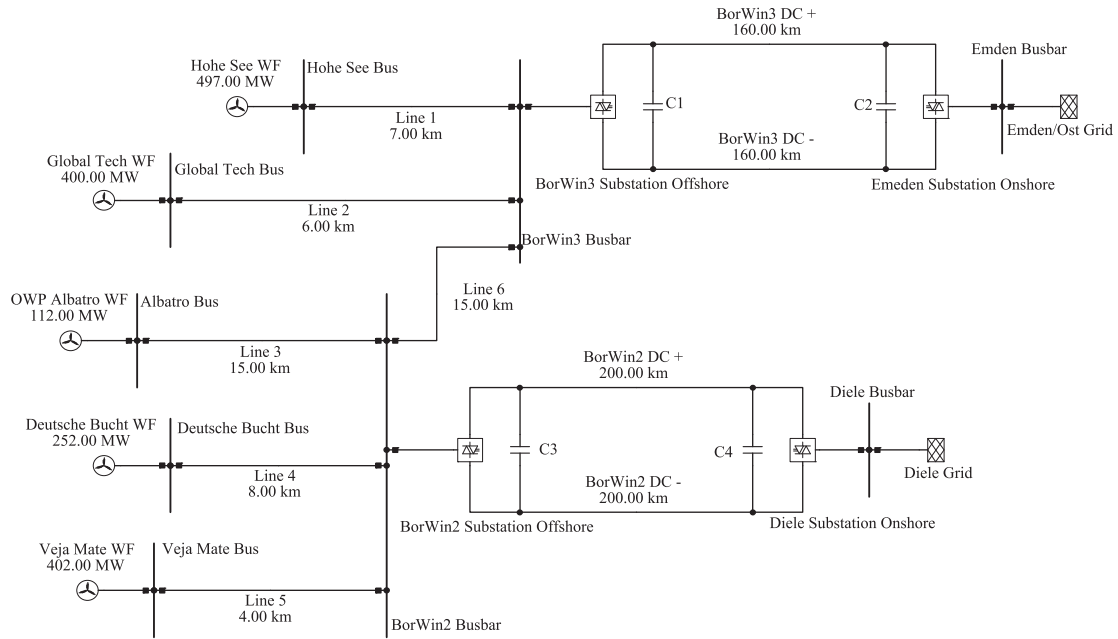


**Figure 7.** Case study: offshore AC network with five offshore wind farms.

i.e.  $\pm 10\%$  in all reactive power management strategies, thus operators can decide the operating point based on active power loss objective function. From the results, it can be concluded that MS4 would be a better reactive power management strategy for optimization. This small example demonstrates that better optimization results can be achieved by selecting suitable reactive power management.

#### 4.2. Offshore AC network with five offshore wind farm:

In the second case study, the proposed methodology is applied on the offshore network with five offshore wind farm as illustrated in Figure 7. The network is derived from the existing and developing offshore wind farm at North Sea. The network considers five offshore wind farms in radial configuration. The internal layout of the wind farms is not the focus of this research, therefore, they are modelled as equivalent power injection sources. The energy from offshore is transferred to onshore using two VSC based HVDC transmission systems. Offshore converters of both transmission systems are in grid-forming mode. The offshore network is formulated by connecting both offshore converters substation busbars with the AC cable. The AC rated voltage of the offshore network is 150.0 kV, and the detail network parameters are given in Appendix.

The rated power for each offshore wind farm is given in Figure 7. The net wind active power in the offshore network is 1663 MW. Thus, the export capacity of each HVDC transmission line is considered as 1700 MW to be able to infeed all energy into each grid according to active power sharing factor ( $\alpha$ ). For the analysis, it is assumed that the onshore grids are strong and have

the capability to receive all the power from the offshore wind farms. In the optimization algorithm, the active power sharing factor can be set from 0.0 to 1.0 where  $\alpha = 1.0$  means all the power is transferred to “Diele” grid and at  $\alpha = 0.0$  all power is exported to “Emden” grid.  $\alpha$  is the input parameter which can be used to limit the active power transport through an HVDC transmission system if the converter capacity is lower than others within the offshore grids. Furthermore, the reactive power sharing factor ( $\beta$ ) is the optimization solution which defines the reactive power contribution of each offshore VSC of HVDC transmission line, where  $\beta = 1.0$  means that the net mismatch reactive power of the network is provided by Borwin2 offshore converter and at  $\beta = 0.0$  the net mismatch reactive power is provided by Borwin3 offshore converter.

The optimization problem is defined using system equations derived in the previous section. The inputs of the algorithm are the wind power infeed, active power sharing factor, and objective function weighting factor. The outputs of the solution are the reactive power set-point of the offshore wind farms, and reactive power sharing factor of HVDC transmission system. The network voltage magnitude, voltage phase angle, VSC active power, and VSC reactive power are the state variables determined by the optimization algorithm. The objective function of the system is set using (5)–(7). AC and DC network topology is defined using (8) and (9). The connection between AC and DC network is completed using (10) and (11). Frequency droop equation given in (1) is applied in all management strategies to apply the active power sharing capability. The relationship between active power sharing factor and frequency droop gain value is completed using (15) and (16). The state variables boundary

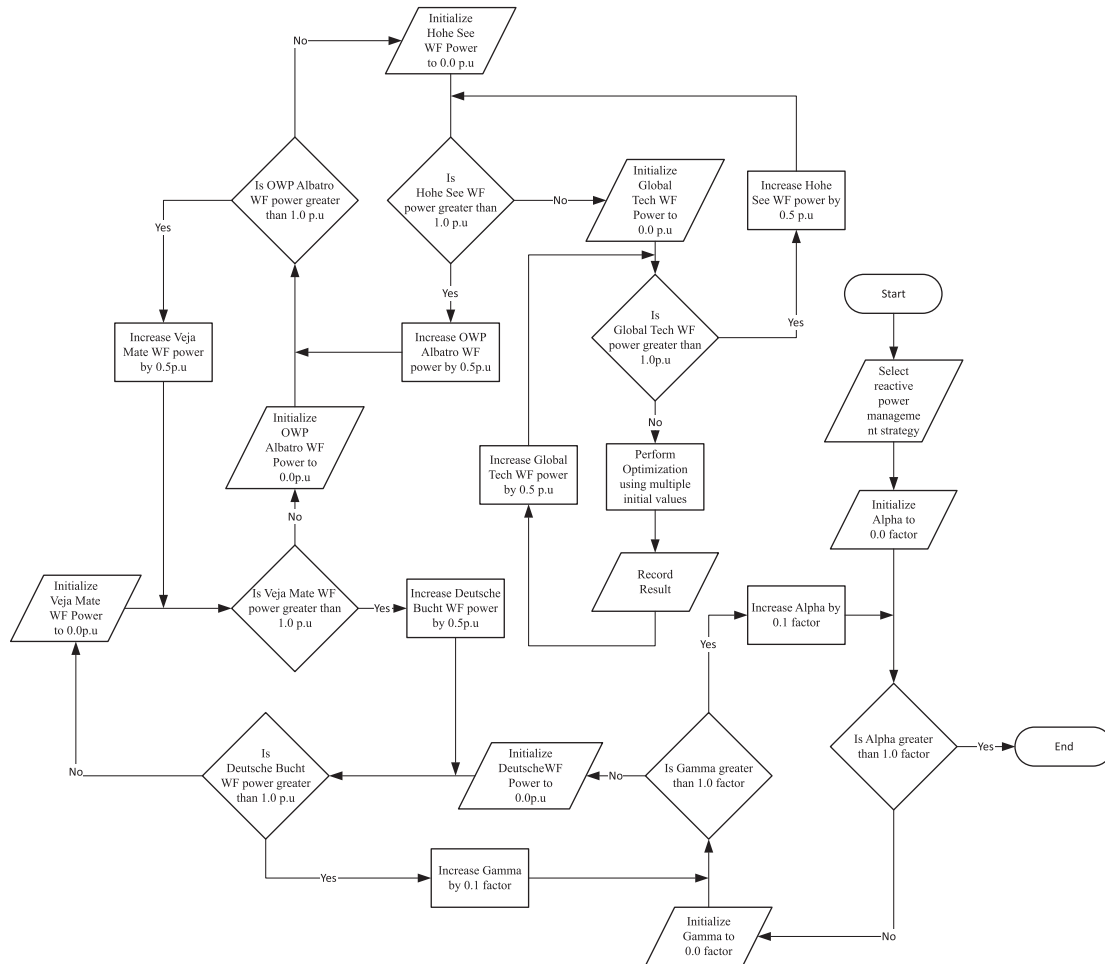
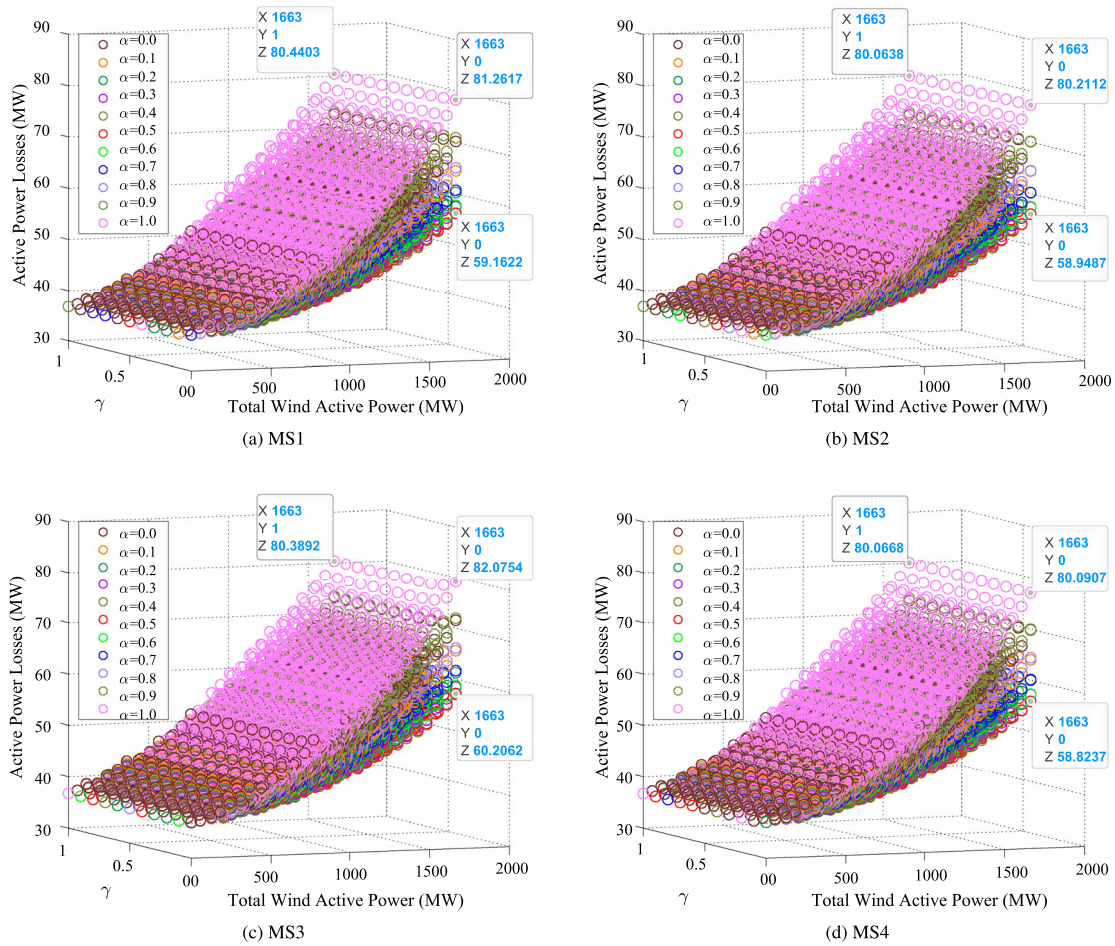


Figure 8. Optimization algorithm flowchart.

limits and maximum frequency condition are applied using (20) and (21). The constraints of reactive power sharing factor and reactive power management strategies are applied using (17) and (19) as well as equations given in Section 3.2.4.

The algorithm performed the steady-state optimization of the offshore grid and it is time independent. The optimum operating point identification depends on the wind speed and the active power sharing between the HVDC transmission system. Three levels of wind speed are considered for each wind farms i.e. low, medium, and high. At low wind speed, the output of the wind farm is considered zero. Offshore wind farms are considered generating 50% of rated power at medium wind speed, and they are set to generate rated power at high wind speed. The output of wind farms is changed sequentially according to wind speed level considering the scale of active power sharing factor and objective function weighting factor. The scale of changing wind speed can be reduced to account for small wind variation, however it will increase the computation time and will require more memory to store the results. Nevertheless, the defined three levels are sufficient to analyse the impact of wind variations on the network. The process flow diagram is shown in Figure 8. The optimization algorithm starts by selecting

the reactive management strategy. Active power sharing is set from  $\alpha = 0.0$  to  $\alpha = 1.0$  with a step change of 0.1 to analyse the effects of export power condition on the network active losses and voltages deviation. Similarly,  $\gamma$  is set from 0.0 to 1.0 with a step change of 0.1 to evaluate the optimization results considering trade-off between both objective functions. Optimization is executed with multiple initial values considering the combination of wind farm active power production i.e. low, medium, and high wind speed. For 29, 403 operating conditions, corresponding optimization results are obtained. The power flow optimization is a nonlinear non-convex problem and it has a large number of local minima. A local minima can be designated as a global minima within the closed interval defined by the constraints and boundaries. The system constraints and limits ensure that the same local minima is found at different initial values for the given predefined conditions and sets of inputs or get no solution at all. Furthermore, global minima that may exist outside the boundaries limits shall be considered as infeasible as it violates the network operational condition such as voltage tolerance limit, converter power capability limit, line thermal loading, wind turbine active and reactive power dispatch limits.



**Figure 9.** Active power losses with respect to net wind power, active power sharing, and objective function weighting factor. (a) MS1. (b) MS2. (c) MS3. (d) MS4.

Active power loss optimization results comparison of four management strategies are shown in Figure 9. The minimum active power losses are achieved at  $\alpha = 0.5$  in all management strategies i.e. when an equal amount of active power is exported to both onshore grids. The highest active power loss would be at  $\alpha = 1.0$ . Among reactive power management strategies, MS4 strategy gives the best optimum solution. The results can be compared at the extreme point i.e. active power loss is 58.8237 MW for  $\gamma = 0.0$  and maximum wind active power. MS2 strategy will produce the maximum active power loss in the network when  $\gamma$  is near zero, and MS1 will provide a worst optimum solution when  $\gamma$  is near 1.0. At  $\alpha = 1.0$  and  $\gamma = 1.0$ , MS1 and MS3 produce about 0.3735 and 0.3224 MW more active power losses respectively in comparison with the MS4 strategy, while MS2 has the same amount of losses as MS4. Note that the offshore AC network is a radial network which gives less provision to optimize the active losses, therefore the difference of the losses among the four strategy is lower but observable. The main point to be observed is how the reactive power management influences the results.

The percentage change in active power losses using MS1, MS2, and MS3 strategies with respect to MS4 strategy is illustrated in Figure 10 at medium wind

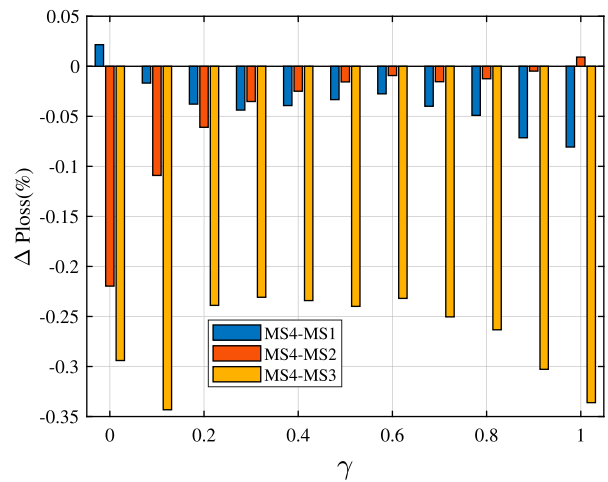


**Figure 10.** Active power losses, when  $\alpha = 0.5$ ,  $P_{wind} = 50\%$ .

power infeed and 50% active power sharing between HVDC transmission system. In comparison, MS3 strategy will produce higher losses i.e. up to 0.35% more. While, MS4 strategy offers more optimized results for almost all values of objective function weightage factor. For  $\gamma = 0.0$ , MS1 provide slightly better results and MS2 strategy at  $\gamma = 1.0$  but the improvement is less than 0.01%. Similarly for the same condition of wind

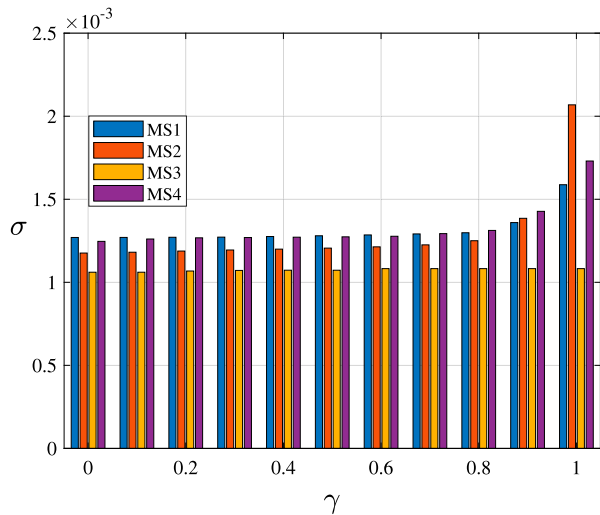


**Figure 11.** Voltages standard deviation when  $\alpha = 0.5, P_{wind} = 50\%$ .

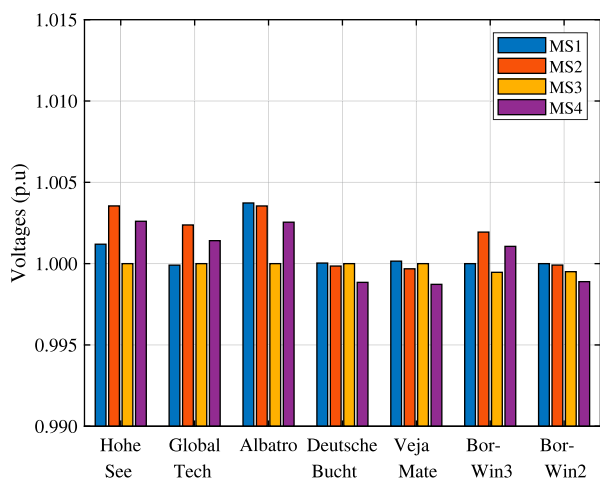


**Figure 12.** Bus voltages when  $\gamma = 1.0, \alpha = 0.5, P_{wind} = 50\%$ .

power infeed and active power sharing, voltage objective function can be compared for all reactive power management strategies as illustrated in Figure 11. The voltage standard deviation with  $\mu = 1.0$  indicates how much network busbars voltage deviate from the rated value. It is obvious that the lowest voltage standard deviation will be achieved with the MS3 strategy since the strategy employs the control of wind turbine busbar voltage to 1.0 p.u and the only change in the voltages occurs at the VSC-HVDC busbars. Moreover, MS1 and MS4 strategies have the same voltage drops in the network for  $\gamma$  value between 0.0 and 0.8, but for  $\gamma = 1.0$ , when only active power loss objective function is optimized, network voltage increases in MS2 and MS4 strategies. Nevertheless, network voltages are still very near to the rated voltage as shown in Figure 12. It can be noticed that the Albatro wind farm busbar has more voltage compared to others due to longer cables, also Hohe See and Global Tech wind farm infeed more reactive power which increases the bus voltage.

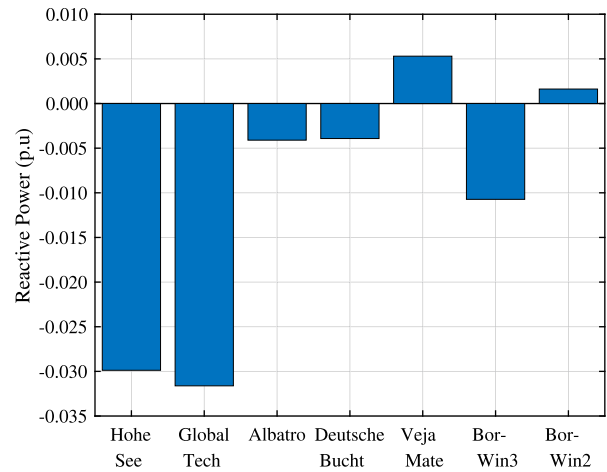


**Figure 13.** Reactive power for MS1 strategy, when  $\gamma = 1.0, \alpha = 0.5, P_{wind} = 50\%$ .

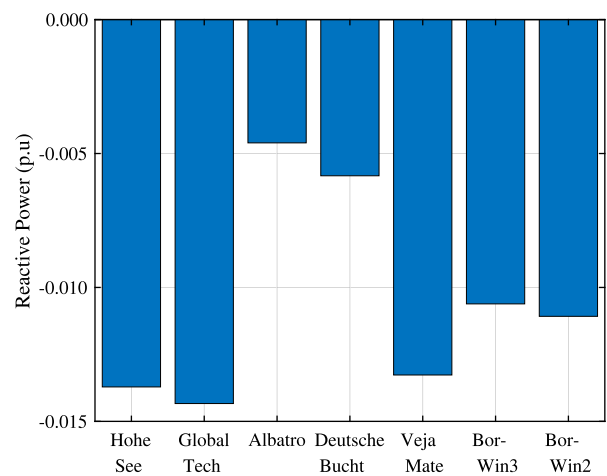


**Figure 14.** Reactive power for MS4 strategy, when  $\gamma = 1.0, \alpha = 0.5, P_{wind} = 50\%$ .

The reactive power infeed comparison between MS1 and MS4 strategies can be made from Figures 13 and 14. Although MS1 strategy has a lower standard deviation of network voltages, it infeeds more inductive reactive power into the network primarily compensating the cable capacitance, and additional capacitive reactive power infeed by VejaMate wind farm and Borwin2 HVDC substation. In this scenario, the reactive power operating points are not suitable since additional capacitive power needs to be compensated by other network elements. On the other hand, MS4 strategy provide reactive power operating point such that it compensates offshore cable capacitance as illustrated in Figure 14.

Offshore AC buses voltage data distribution is shown in Figure 15 using box-plot. Here, equal active power is transmitted through both HVDC transmission lines, and the optimization solution is acquired at  $\alpha = 0.5$  and  $\gamma = 0.5$ . In MS1 strategy, the bus voltages of Borwin3 and Borwin2 substation are controlled to 1.0 p.u while the voltages at other busbars result according to active and reactive power flow in the network. In this

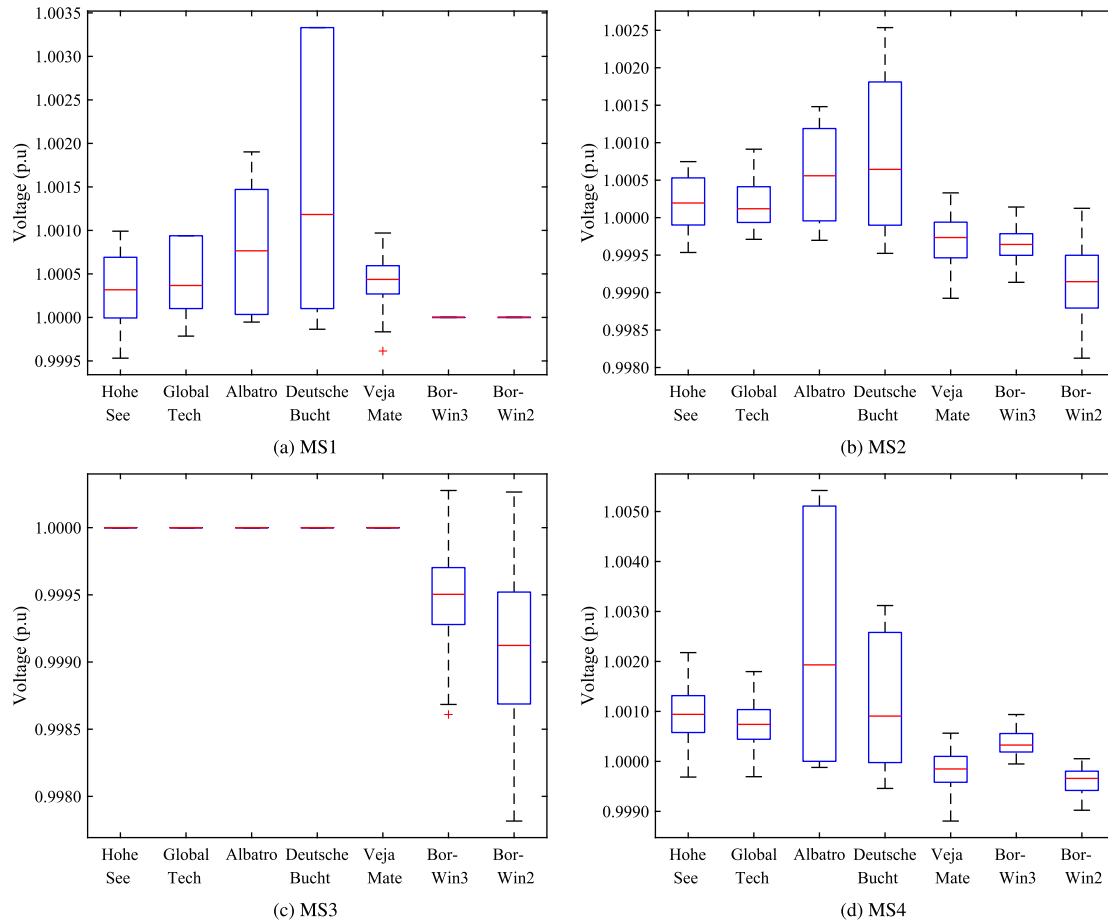


**Figure 15.** Offshore busbar voltage profile at  $\alpha = 0.5$  and  $\gamma = 0.5$ . (a) MS1. (b) MS2. (c) MS3. (d) MS4.

strategy, the optimized operation is achieved by controlling offshore wind farm reactive power only. Voltages at Deutsche Bucht and Albatro offshore wind farm busbar are higher since they are injecting maximum reactive power into the network and reaches their operational limits. In MS2 strategy, droop scheme changes the converter busbars and enables the control over the reactive power contribution by both offshore VSCs of HVDC transmission systems. It can be observed that the mean voltage deviation from the rated value at the Albatro and Deutsche Bucht busbars is reduced. Further, optimization with fixed PCC bus voltage (MS3) of offshore wind farm requires more reactive power to be supplied by the wind turbine as shown in Figure A1. In comparison between MS2 and MS4 strategies, the voltage variation on the VSC controlling busbar in MS4 strategy is less while the mean value on the offshore wind farm substation PCC bus is lower in MS2 strategy.

The response of reactive power infeed by offshore wind farm at their PCC bus and VSCs of HVDC transmission system is shown in Figure A1. These optimization results are obtained at  $\alpha = 0.5$  and  $\gamma = 0.5$ . Other results over the full range of  $\alpha$  and  $\gamma$  can be obtained in the similar manner. The generator-oriented sign convention is applied. In MS1 strategy, wind farm Albatro and Deutsche Bucht are injecting inductive reactive power at their maximum limits. In MS3

strategy, offshore wind farms are required to infeed more than their reactive power limits in order to control the fixed voltages at their PCC busbar. Furthermore, the mean reactive power contribution by offshore VSCs are approximately the same in MS4 strategy i.e. both VSC contribute equally in average to compensate reactive power hereby maximizing active power transfer.

In Figure A2 Pareto Front analysis at full wind power infeed and  $\alpha = 0.5$  is shown for the best optimum solution with respect to the objective function weighted factor ( $\gamma$ ). It can be observed that the optimum solution tends to move toward either at active power loss or voltage deviation functions depending on the reactive power management strategy. Obviously, there is less provision in regulating the network voltages in MS3 strategy therefore both objective functions are not optimized significantly over the range of  $0.1 \leq \gamma \leq 1.0$ . It is of no significance to apply multiple objective functions for optimization rather only active power loss objective function will be sufficient in case of MS3 strategy. In MS2 strategy, the optimal point stands more toward active power loss function and small improvement can be seen in the voltage over the range of  $0.0 \leq \gamma \leq 0.9$ . However, the difference in the optimized result is more at  $\gamma = 1.0$  and  $\gamma = 0.0$  in comparison to the MS3 strategy. In MS1 and MS2, the Pareto points are evenly distributed and there is a provision to select

optimal operating points according to trade-off criteria. Furthermore, the response also indicates that the voltage deviation in the MS1 strategy is higher compared to MS4 i.e. the voltage least square error is  $0.95 \times 10^{-4}$  in MS4 where as  $1.05 \times 10^{-4}$  in MS1 at  $\gamma = 0.0$ . When  $\gamma = 1.0$  then MS4 is also optimized at a lower value of  $1.35 \times 10^{-4}$  where as in MS1 the voltage least square error is  $1.40 \times 10^{-4}$ . The analysis shows that the MS4 strategy provides more optimized results compared to other reactive power management strategies. The reactive power control strategy in MS4 ensures that any additional reactive power change due to reference bus voltage must be exchanged among converters hereby reduces voltage deviation. Thus, voltage and active power losses are optimized simultaneously to some extent.

## 5. Conclusion and recommendation

In this article, concept of offshore AC hub is addressed in which large scale offshore wind farms are integrated together hereby formulating an offshore AC network. The combined energy is transported from this network to onshore using a VSC-HVDC transmission system. Offshore HVDC converters are operating in parallel using voltage and frequency droop schemes. The droop schemes give an additional degree of freedom to control sharing of power between HVDC converters and provide more variables for optimization. However, more constraints are required for power management with the increase of optimization variables, and the correlation between variables needs to be defined for better network operation. The article compares four different reactive power management strategies to analyse the optimization solution. It is found that the reactive power control criteria affects the objective function minimization. The study demonstrates that the solution is less optimized when there are no additional reactive power constraints i.e. MS1 case. The study considers two objective functions i.e. voltage deviation minimization and active power loss minimization. Both objective functions are conflicting in nature. Also, if busbar voltage control constraint (MS3 case) is applied then the network mainly optimizes for voltage deviation. The study suggests to apply the MS4 strategy to obtain the offshore AC network optimum operating point since it produces lowest active power losses and lower voltage deviation in the network. With the proposed optimization method, the desired frequency and voltage droop gains value, reactive power sharing among HVDC offshore converter, and wind farm reactive power set-points can be calculated for the offshore grid. Future work could investigate the network optimization considering the probabilistic nature of wind speed and reactive power compensation cost objective functions. Furthermore, the proposed optimization method can be applied to study future offshore wind farm projects.

## Disclosure statement

No potential conflict of interest was reported by the author(s).

## ORCID

Muhammad Raza  <http://orcid.org/0000-0002-4385-5020>

## References

- [1] Selot F, Fraile D, Brindley G, et al. Offshore wind in Europe: key trends and statistics 2018. Brussels: WindEurope; 2019 Feb. (Tech. Rep.).
- [2] Marten A-K, Akmatov V, Sørensen TB, et al. Kriegers flak-combined grid solution: coordinated cross-border control of a meshed HVAC/HVDC offshore wind power grid. *IET Renew Power Gener.* 2018 Oct;12(13):1493–1499.
- [3] Decker JD, Kreutzkamp P. Offshore electricity grid infrastructure in Europe: a techno-economic assessment. Brussels: OffshoreGrid (3E Coordinator); 2011 Oct. (Tech. Rep.). Available from: <http://www.offshoregrid.eu/>
- [4] Brouwers J. TenneT News: Tennet presents Hub and Spoke concept for large scale wind energy on the North Sea; 2016 Jun.
- [5] Maria K, Hoerchens U. Offshore Netzentwicklungsplan 2030. Grid Development Plan Power; 2017 May. (Tech. Rep.). Available from: [www.netzentwicklungsplan.de](http://www.netzentwicklungsplan.de)
- [6] Wang P, Lu X, Wang W, et al. Frequency division based coordinated control of three-Port converter interfaced hybrid energy storage systems in autonomous DC microgrids. *IEEE Access.* 2018;6:25389–25398.
- [7] Leon AE. Short-term frequency regulation and inertia emulation using an MMC-based MTDC system. *IEEE Trans Power Syst.* 2018 May;33(3):2854–2863.
- [8] Li Y, Xu Z, Ostergaard J, et al. Coordinated control strategies for offshore wind farm integration via VSC-HVDC for system frequency support. *IEEE Trans Energy Convers.* 2017 Sep;32(3):843–856.
- [9] Zhang L, Tang Y, Yang S, et al. Decoupled power control for a modular-multilevel-converter-based hybrid AC-DC grid integrated with hybrid energy storage. *IEEE Trans Ind Electron.* 2019 Apr;66(4):2926–2934.
- [10] Li H, Liu C, Li G, et al. An enhanced DC voltage droop-control for the VSC-HVDC grid. *IEEE Trans Power Syst.* 2017 Mar;32(2):1520–1527.
- [11] Sandano R, Farrell M, Basu M. Enhanced master/slave control strategy enabling grid support services and offshore wind power dispatch in a multi-terminal VSC HVDC transmission system. *Renew Energy.* 2017 Dec;113:1580–1588.
- [12] Chuangpishit S, Tabesh A, Moradi-Sharbabk Z, et al. Topology design for collector systems of offshore wind farms with pure DC power systems. *IEEE Trans Ind Electron.* 2014 Jan;61(1):320–328.
- [13] Musasa K, Nwulu NI. A novel concept for offshore wind-power plant with DC collection system based on radial-connected converter topology. *IEEE Access.* 2018;6:67217–67222.
- [14] Musasa K, Nwulu NI, Gitau MN, et al. Review on DC collection grids for offshore wind farms with high-voltage DC transmission system. *IET Power Electron.* 2017 Dec;10(15):2104–2115.

- [15] Yang R, Shi G, Cai X, et al. Voltage source control of offshore all-DC wind farm. *J Eng.* 2019 Jul;2019(18):4718–4722.
- [16] Paez JD, Frey D, Maneiro J, et al. Overview of DC–DC converters dedicated to HVdc grids. *IEEE Trans Power Deliv.* 2019 Feb;34(1):119–128.
- [17] Yin R, Shi M, Hu W, et al. An accelerated model of modular isolated DC/DC converter used in offshore DC wind farm. *IEEE Trans Power Electron.* 2019 Apr;34(4):3150–3163.
- [18] Guan M. A series-connected offshore wind farm based on modular dual-active-bridge (DAB) isolated DC–DC converter. *IEEE Trans Energy Convers.* 2019 Sep;34(3):1422–1431.
- [19] Krishnamoorthy H, Daniel M, Ramos-Ruiz J, et al. Isolated AC–DC converter using medium frequency transformer for off-Shore wind turbine DC collection grid. *IEEE Trans Ind Electron.* 2017 Nov;64(11):8939–8947.
- [20] Jovic D, Taherbaneh M, Taisne J-P, et al. Offshore DC grids as an interconnection of radial systems: protection and control aspects. *IEEE Trans Smart Grid.* 2015 Mar;6(2):903–910.
- [21] Gomis-Bellmunt O, Liang J, Ekanayake J, et al. Topologies of multiterminal HVDC-VSC transmission for large offshore wind farms. *Electric Power Syst Res.* 2011 Feb;81(2):271–281.
- [22] Raza M, Peñalba MA, Gomis-Bellmunt O. Short circuit analysis of an offshore AC network having multiple grid forming VSC-HVDC links. *Int J Electrical Power Energy Syst.* 2018 Nov;102:364–380.
- [23] Wang X, Li L, Palazoglu A, et al. Optimization and control of offshore wind farms with energy storage systems. *IFAC-PapersOnLine.* 2018 Jan;51(18):862–867.
- [24] Raza M, Collados C, Gomis-Bellmunt O. Reactive power management in an offshore AC network having multiple voltage source converters. *Appl Energy.* 2017 Nov;206:793–803.
- [25] Raza M. Active and reactive power control of hybrid offshore AC and DC grids. *Automatika.* 2019 Oct;60(4):432–442.
- [26] Hou P, Enevoldsen P, Hu W, et al. Offshore wind farm repowering optimization. *Appl Energy.* 2017 Dec;208:834–844.
- [27] Mohamed MA, Abdullah HM, Al-Sumaiti AS, et al. Towards energy management negotiation between distributed AC/DC networks. *IEEE Access.* 2020;8:215438–215456.
- [28] Mohamed MA, Jin T, Su W. An effective stochastic framework for smart coordinated operation of wind park and energy storage unit. *Appl Energy.* 2020 Aug;272:115228.
- [29] Jin T, Chen Y, Guo J, et al. An effective compensation control strategy for power quality enhancement of unified power quality conditioner. *Energy Rep.* 2020 Nov;6:2167–2179.
- [30] Wang N, Li J, Hu W, et al. Optimal reactive power dispatch of a full-scale converter based wind farm considering loss minimization. *Renew Energy.* 2019 Feb;139:292–301.
- [31] Schönleber K, Collados C, Pinto RT, et al. Optimization-based reactive power control in HVDC-connected wind power plants. *Renew Energy.* 2017 Aug;109:500–509.
- [32] Kotur D, Stefanov P. Optimal power flow control in the system with offshore wind power plants connected to the MTDC network. *Int J Electrical Power Energy Syst.* 2019 Feb;105:142–150.
- [33] Aragüés-Peñalba M, Sau Bassols J, Galceran Arellano S, et al. Optimal operation of hybrid high voltage direct current and alternating current networks based on OPF combined with droop voltage control. *Int J Electrical Power Energy Syst.* 2018 Oct;101:176–188.
- [34] Ghaljehei M, Soltani Z, Lin J, et al. Stochastic multi-objective optimal energy and reactive power dispatch considering cost, loading margin and coordinated reactive power reserve management. *Electric Power Syst Res.* 2019 Jan;166:163–177.
- [35] Bian Z, Xu Z, Xiao L, et al. Selection of optimal access point for offshore wind farm based on multi-objective decision making. *Int J Electrical Power Energy Syst.* 2018 Dec;103:43–49.
- [36] Alonso M, Amaris H, Alvarez-Ortega C. A multiobjective approach for reactive power planning in networks with wind power generation. *Renew Energy.* 2012 Jan;37(1):180–191.
- [37] Mohseni-Bonab SM, Rabiee A. Optimal reactive power dispatch: a review, and a new stochastic voltage stability constrained multi-objective model at the presence of uncertain wind power generation. *IET Gener, Transm Dis.* 2017 Mar;11(4):815–829.
- [38] Junge C. Borwin 2: grid connection of the great class; 2017.
- [39] Raza M, Prieto-Araujo E, Gomis-Bellmunt O. Small-signal stability analysis of offshore AC network having multiple VSC-HVDC systems. *IEEE Trans Power Deliv.* 2018 Apr;33(2):830–839.
- [40] Beerten J, Cole S, Belmans R. Generalized steady-state VSC MTDC model for sequential AC/DC power flow algorithms. *IEEE Trans Power Syst.* 2012 May;27(2):821–829.
- [41] ABB. Product catalogue: XLPE submarine cable systems; 2017.

## Appendix

Offshore grid parameters and offshore wind farm rated values are given in this section.

**Table A1.** Cable parameters.

Name	Type	No. of cables	Length (km)
Line 1	Type-II	3	7
Line 2	Type-III	2	6
Line 3	Type-I	1	15
Line 4	Type-I	2	8
Line 5	Type-III	2	4
Line 6	Type-III	2	15
Borwin3 DC	Type-IV (Bi-Pole)	1	160
Borwin2 DC	Type-IV (Bi-Pole)	1	200

**Table A2.** Cable type data [41].

Name	Type	Rated voltage kV	Resistance $\Omega$ /km	Inductance mH/km	Capacitance $\mu$ F/km	Cross-section $\text{mm}^2$
Type-I	AC	150.0	0.099	0.44	0.14	300
Type-II	AC	150.0	0.033	0.40	0.17	500
Type-III	AC	150.0	0.022	0.37	0.21	800
Type-IV	DC	320.0	0.0073			2400

**Table A3.** Converter and wind farm parameters.

<b>HVDC Transmission</b>	
Nominal Voltage ( $u_{ac}, u_{dc}$ )	150 kV, $\pm 320$ kV
Converter (topology, $S_{rt}, \cos \theta$ )	MMC, 1700 MVA, $\pm 0.9$
Converter No-load Coefficient (a)	$11.033 \times 10^{-3}$ p.u
Converter Voltage Drop Coefficient (b)	$3.464 \times 10^{-3}$ p.u
Converter Ohmic-loss Coefficient (c)	$4.400 \times 10^{-3}$ p.u
<b>Wind Farms</b>	
Hohe See ( $P_{rt}, u_{ac}, \cos \theta$ )	497 MW, 150 kV, $\pm 0.98$
Global Tech ( $P_{rt}, u_{ac}, \cos \theta$ )	400 MW, 150 kV, $\pm 0.98$
Albatro ( $P_{rt}, u_{ac}, \cos \theta$ )	112 MW, 150 kV, $\pm 0.98$
Deutsche Bucht ( $P_{rt}, u_{ac}, \cos \theta$ )	252 MW, 150 kV, $\pm 0.98$
Veja Mate ( $P_{rt}, u_{ac}, \cos \theta$ )	402 MW, 150 kV, $\pm 0.98$
<b>Onshore Grid</b>	
Diele ( $u_{ac}$ )	380 kV
Emden/Ost ( $u_{ac}$ )	380 kV

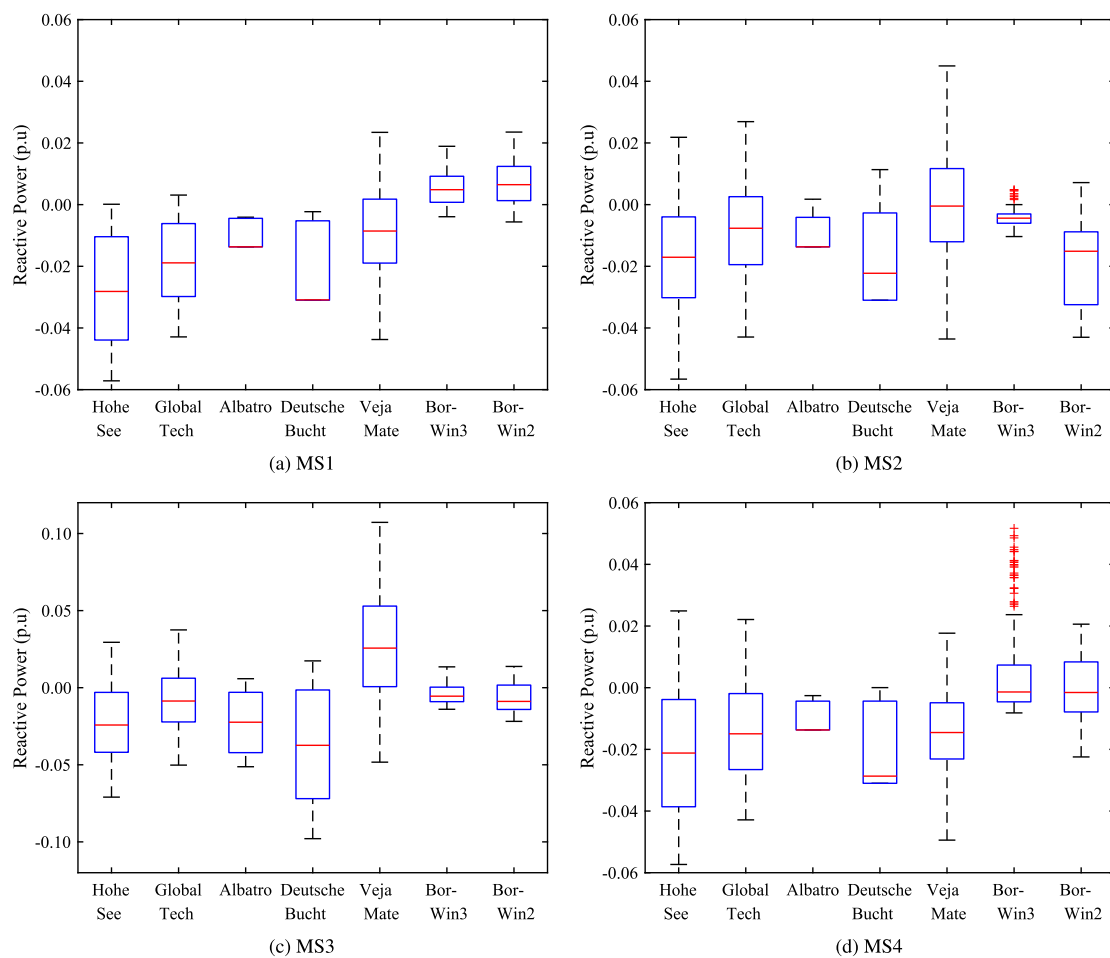


**Figure A1.** Reactive power contribution by each source at  $\alpha = 0.5$  and  $\gamma = 0.5$ . (a) MS1. (b) MS2. (c) MS3. (d) MS4.

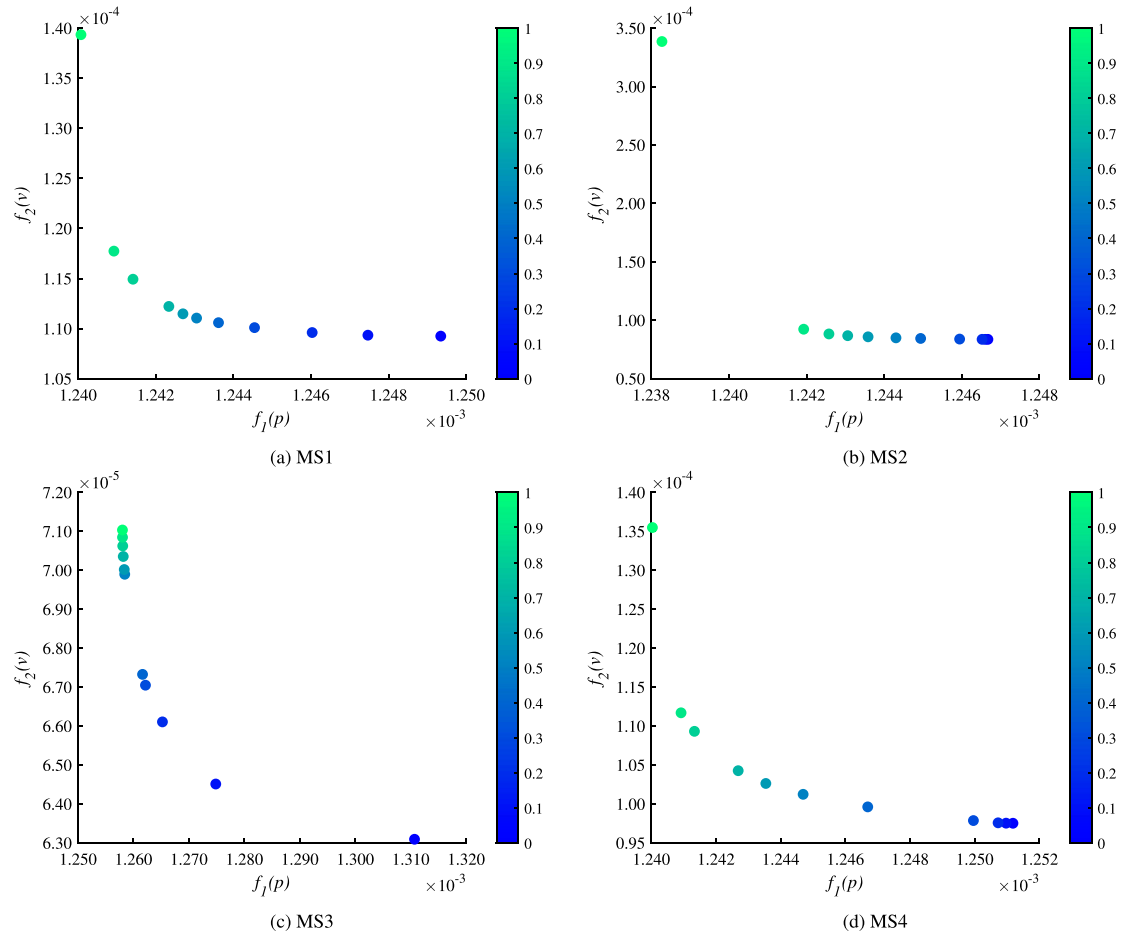


**Figure A2.** Pareto front analysis at full wind power and  $\alpha = 0.5$ . (a) MS1. (b) MS2. (c) MS3. (d) MS4.